PAPER

Electrically pumped photonic crystal laser constructed with organic semiconductors

IOP Publishing | Astro Ltd
Laser Physics
Laser Phys. **27** (2017) 035801 (6pp)
doi:10.1088/1555-6611/aa5291

Electrically pumped photonic crystal laser constructed with organic semiconductors

Yuan-yuan Cai[1,2], Xiao Chen[1], Ning Li[1], Chang-wei Li[1] and Yi-quan Wang[1]

[1] College of Science, Minzu University of China, Beijing 100081, People's Republic of China
[2] School of Science, Beijing Jiaotong University, Beijing 100044, People's Republic of China

E-mail: xchen4399@126.com

Received 27 October 2016
Accepted for publication 2 December 2016
Published 13 January 2017

Abstract

We experimentally demonstrate the lasing action of electrically pumped octagonal quasi-crystal microcavities formed in a layer of conjugated polymer poly[2-methoxy-5-(2-ethylhexyloxy)-1,4-phenylenevinylene] (MEH-PPV) sandwiched between two electrodes. Lasing from a point-defect microcavity is observed at a wavelength of 606 nm with a narrow linewidth of 0.5 nm, limited by the spectrometer resolution. Due to the properties of the photonic bandgap and localization in photonic crystals, the threshold current for lasing is low at 0.8 mA. The ion injection in the luminescent polymer layer by focused ion beam (FIB) etching technology also contributes to enhancement of the carrier density as well as the mobility, resulting in an increase of MEH-PPV conductivity and a decrease of turn-on voltage.

Keywords: laser, photonic crystal, organic semiconductor, electrical pumping

(Some figures may appear in colour only in the online journal)

1. Introduction

Photonic crystals (PhCs) have been proposed as periodic optical nanostructures in the last century, attracting great interest, and considerable progress has been made in both fundamental research and applications. Based on the photonic bandgaps effect, various passive and active PhCs devices with different lattices, symmetries and structures have been widely investigated [1]. For example, some basic PhC components such as routers, filters and couplers have demonstrated considerable potential in optical communication. Due to the high density of states at band edges and the nonlinear property of the materials, PhC control devices like optical switches and wavelength converters have opened up the prospect of application in all-optical networks and optical logic calculation. In addition, ultralow-threshold ultrasmall PhC lasers with high-quality (Q-factor) microcavities have become another promising research avenue since Painter first introduced a photonic bandgap defect-mode laser in 1999 [2–6]. Photonic crystals, compared with other microstructures utilized in lasers are an ideal candidate for flexibility in tuning of the symmetry, frequency and localization property of defects, thus demonstrating excellent ability for the manipulation of light and the modulation of spontaneous emission [7–9].

Materials development has also played another crucial role in the progress of new lasers. A variety of novel semiconducting materials used as gain media have been utilized to further improve the light-emitting performance in PhCs, including inorganic and organic materials [10–13]. Conjugated polymers combine remarkable optoelectronic properties with simple fabrication and tailoring of the structure to give the desired functions. They also provides a means to enhance the interaction between photons and electronic excitations, so that it is beneficial for higher efficiency and brightness in lasers and numerous other new devices [14–18].

Although polymer semiconductors have excellent optoelectronic performance, organic photonic crystal lasers, to date, still present a big challenge. The low refractive index of organic materials makes it difficult to obtain effective bandgaps in ordinary periodic PhC structures. Quasi-periodic photonic crystals (QPCs), however, have been proven to offer more flexibility in modifying optical characteristics and allow a smaller dielectric constant necessary for complete photonic bandgaps due to the higher rotation symmetry and long-range order [19–21]. As the symmetry increases, the QPC Brillouin zone becomes more circular, and is thus more favorable for achieving better complete photonic bandgaps. Furthermore, under current micromachining accuracy, it is easy to achieve

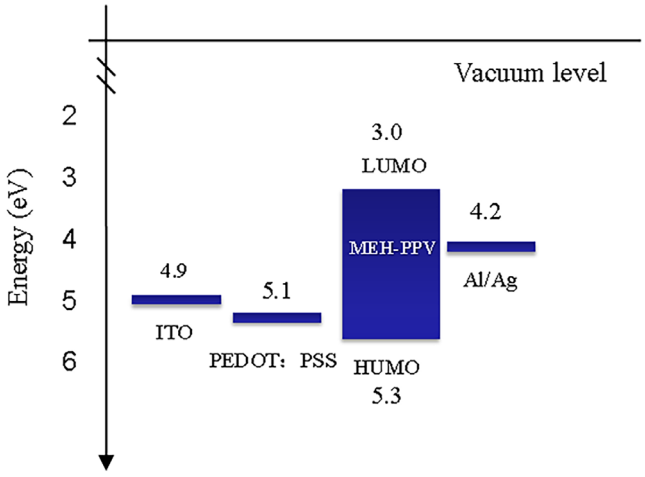

Figure 1. Energy-level diagram of the heterostructure ITO/PEDOT: PSS/MEH-PPV/Al/Ag in light-emitting devices.

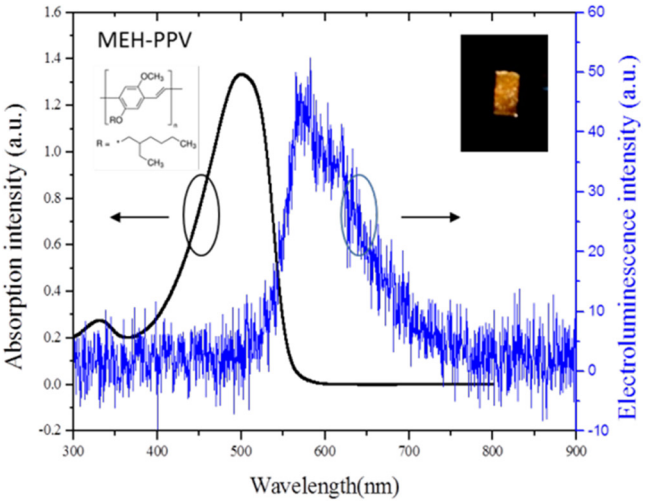

Figure 2. Electroluminescence spectrum of the MEH-PPV film with turn-on voltage of 14 V and the corresponding absorption spectrum detected by a spectrophotometer. The left inset is the chemical structure of MEH-PPV, and the right inset is the EL photo of MEH-PPV without PC microcavity.

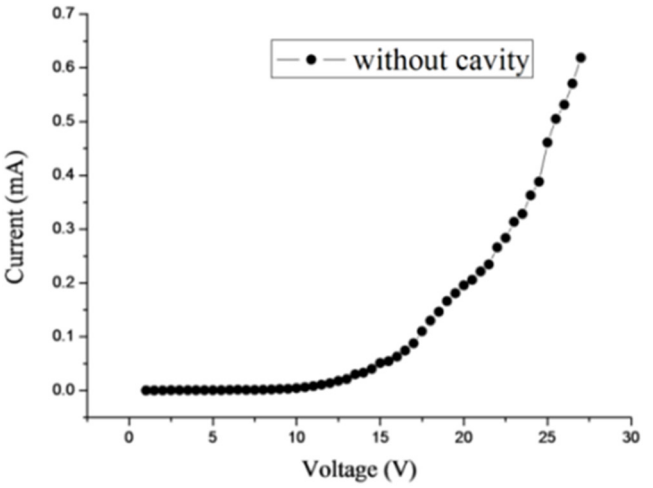

Figure 3. Measured *I–V* characteristics of organic device without PhC microcavity.

bandgaps with octagonal QPCs in the visible band, covering the luminescent spectrum of organic semiconductors. The combination of polymers and quasi-periodic structures, therefore, provides better active layers, higher efficiency and more uniform in-plane confinement in all directions for light-emitting devices. And more importantly, the photonic crystal waveguide formed by a defect microcavity is capable of intensively collecting certain modes of photons and trapping them inside, resulting in light amplification. In [22], we have proved the lasing action in conjugated polymer poly{[2-[2′,5′-bis(2″-ethylhexyloxy)phenyl]-1,4-phenylenevinylene]-co-[2-methoxy-5-(2′-ethylhexyloxy)-1,4-phenylenevinylene]} (BEHP-PPV)-co-(MEH-PPV) based on an octagonal quasi-crystal microcavity structure under excitation by 355 nm/30 ps Nd: YAG pulses. In comparison, electrically driven lasers may offer better prospects for commercial applications because of easy integration and low cost. The purpose of this article is to present the design and fabrication of an electrically pumped laser with a QPC microcavity patterned on a conjugated polymer poly[2-methoxy-5-(2-ethylhexyloxy)-1,4-phenylenevinylene] (MEH-PPV) layer. The experiment results show the lasing is observed at 606 nm with a full width at half maximum (FWHM) of 0.5 nm. The threshold current for lasing is around 0.8 mA.

2. Design and simulation

For light-emitting devices, the typical conductive light-emitting material MEH-PPV is chosen as the gain medium. Modified indium tin oxide (ITO) on the glass processed by wet-etch technology is used as an anode bar and the substrate of MEH-PPV. An Al bar is used as a cathode and Ag is deposited on the top of MEH-PPV layer by magnetron sputtering technology for protection, respectively. The conductive area is the cross section (2 mm × 2 mm) between two electrodes. In order to make the ITO surface smooth for the prevention of electrical shots and reducing the turn-on voltage, a layer of PEDOT: PSS (poly(3,4-ethylenedioxythiophene)-poly (styrenesulfonate)) is spin-coated on the ITO, thus extending the lifetime of devices. Moreover, the PEDOT: PSS layer aligns the Fermi level of the ITO with MEH-PPV as closely as possible for efficient hole-state injection. Figure 1 illustrates the energy-level diagram of the device heterostructure ITO/PEDOT: PSS/MEH-PPV/Al/Ag. This energy-band distribution makes the carrier injection and transport easier, as well as the exciton formation within the luminescent layer under a certain voltage.

In the structure, the thickness of the MEH-PPV film is controlled to be 200 nm and the refractive index is about 1.77. The electroluminescence (EL) spectrum of the MEH-PPV film is depicted in figure 2, which exhibits a broad emission in the 550–650 nm range with a FWHM of ~100 nm. A large Stokes shift of about 100 nm shows between the peaks of EL and the absorption spectrum (400–550 nm), thus effectively suppressing the EL self-absorption and reducing the lasing threshold. Figure 3 shows the measured voltage–current characteristics of this device with a turn-on voltage of 14 V.

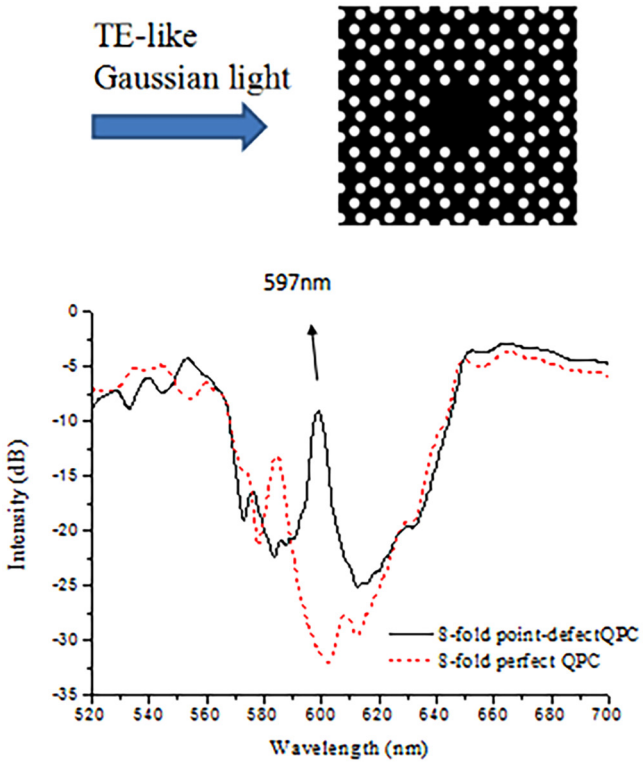

Figure 4. Transmission spectrum of eightfold organic quasi-crystal slab with (without) a microcavity. Transverse electric (TE) modes: there is no electric field in the direction of propagation, only a magnetic field along the direction of propagation.

According to the EL spectrum, we designed quasi-periodic photonic crystal microcavities. We balanced the effect of rotation symmetry on the bandgaps and the difficulty in the etching process, and finally chose an octagonal quasi-crystal to achieve the desired bandgaps. This eightfold symmetry pattern is tiled by squares and rhombuses with an acute angle of 45°. Using the finite-difference time-domain (FDTD) method, the PhC structure parameters of the MEH-PPV slab were optimized as follows: the lattice constant $a = 270$ nm, air-rod radius $r = 65$ nm, and slab thickness $d = 200$ nm. The transmission spectrum in figure 4 demonstrates the complete bandgap of MEH-PPV covers the range from 565 nm to 645 nm, matching its EL spectrum. A defect microcavity is introduced into the QPC slab by removing the central nine air rods, so that it exhibits a localized defect mode at $\lambda = 597$ nm, close to the EL peak.

In order to further investigate the photon modulation by an octagonal QPC microcavity at a low refractive index, we set a point source at a wavelength 597 nm at different locations, as shown in figure 5. It reveals that no matter where the source is, the emitted photons in any direction in plane have nowhere else to go, but are trapped in the point-defect 'well' when the light frequencies match with those of defect modes supported by a microcavity. This microcavity has a high-photon density of states inside, so that it captures sufficient photons and strongly localizes them in the defect region. This effect results in light amplification in the cavity. Those photons cannot escape in-plane, but have to propagate in a vertical along the organic defect waveguide. Between the Al/Ag electrode and the ITO-glass/air surface, certain light modes supported by the microcavity will be further amplified and finally output as a collimated light source.

3. Experiments

Based on the simulation, we adopted an FIB etching system as a micro/nano-processing tool for transferring the design patterns onto the organic MEH-PPV device. A Ga^+ ion beam generated by a Canion ion gun was connected to the ultra-high vacuum chamber, where the sample was placed. A spot current of 30 pA was obtained from a weak emission current of 1 μA at 25 KeV. A weak current can reduce the sample damage and the Gaussian wings of ion beams. The scanning electron microscopy image of the PhC microcavity is shown in figure 6. The total etched area is about 20 μm × 20 μm with 516 air rods inside. Figure 7 shows the experiment setup for detecting the electroluminescence. The results in figure 8 demonstrate that the spectral emission from the PhC microcavity is significantly narrowed and the intensity is greatly enhanced as the injection current increases. The defect mode occurs at $\lambda = 606$ nm with an FWHM of ~0.5 nm, only limited by the resolution of the fiber spectrometer (Ocean Optics QE65000 with a resolution of 0.5 nm). Furthermore, the amplified spontaneous emission (ASE) from an MEH-PPV waveguide is also detected for comparison. The linewidth of the ASE shown in the inset of figure 8 is around 10 nm: 20 times the magnitude (or more) of that for the defect mode. The wavelength of the defect mode red-shifts 9 nm compared with the simulated results. This is mainly caused by the interaction between quasi-crystal structures and the ASE of MEH-PPV. In addition, the measurement error of the film thickness and the etching error in FIB processing (etching resolution of the FIB is 10 nm) can also make the differences between the measured spectrum and simulated results.

The dependence of output intensity on the applied current is displayed in figure 9. A distinct slope change is observed at the lasing threshold 0.8 mA. Below the threshold, the light coupled-out vertically from the microcavity is a wide spectrum and the shape of spectrum is independent of the applied current, which is a characteristic of spontaneous emission from the MEH-PPV film. At 0.8 mA, an abrupt narrowing in the output spectrum is observed as almost all the emission power is coupling into the lasing modes (λ ~ 606 nm). With further increase in the current, the output spectrum is completely dominated by the narrow lasing spectral peak. The lasing threshold under electrical pumping is approximately 0.8mA, which is a low value. This is not surprising because photonic crystals have the potential to realize threshold-less lasing operation and allow a single mode in the transition spectrum due to their excellent ability to modulate the emission rate and localization of photons in microcavities [2]. The lasing threshold in our experiment is mainly due to the consumption at electrodes.

To understand the properties of laser light, it is important to know how the laser is generated. Laser, a coherent light (both spatially and temporally) is the combination of photons with the same mode along the same direction. To realize

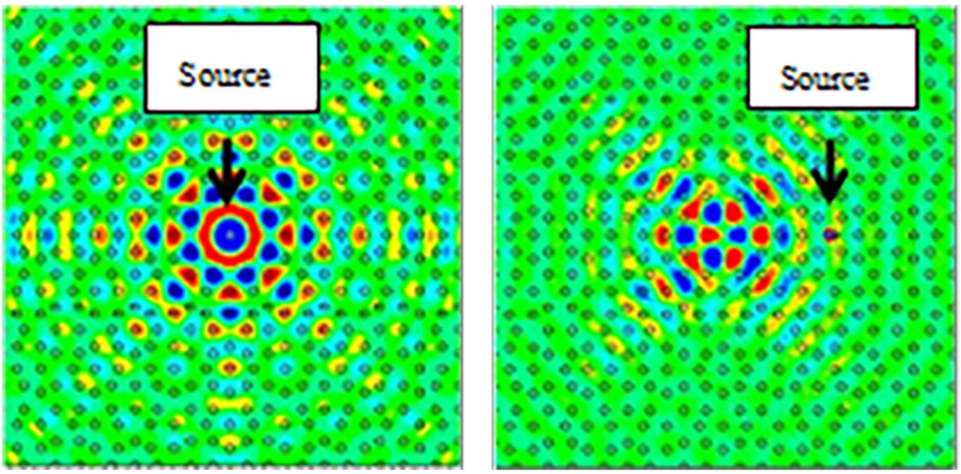

Figure 5. Photon capture in quasi-crystal microcavity. Left: a point light source in the defect center; right: a point light source in the vicinity of the defect.

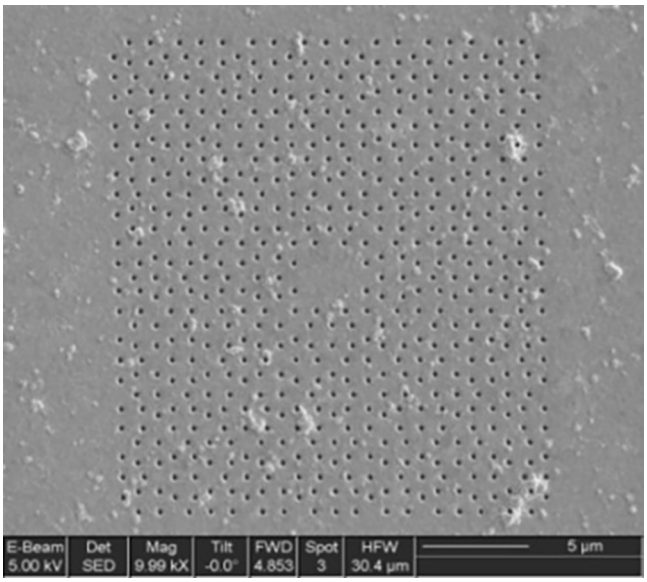

Figure 6. SEM picture of eightfold QPC microcavity on organic slab.

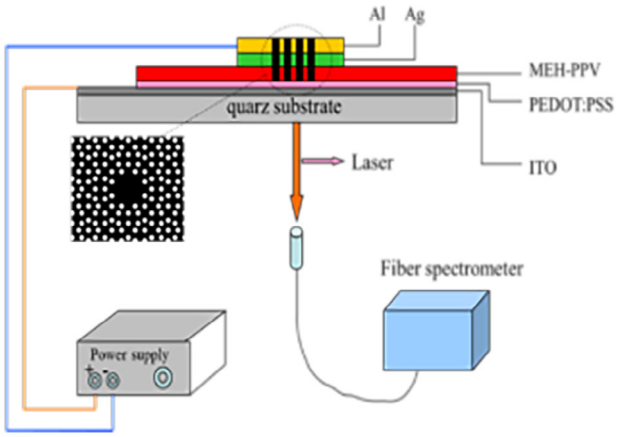

Figure 7. Schematic diagram of electrically pumped quasi-crystal laser.

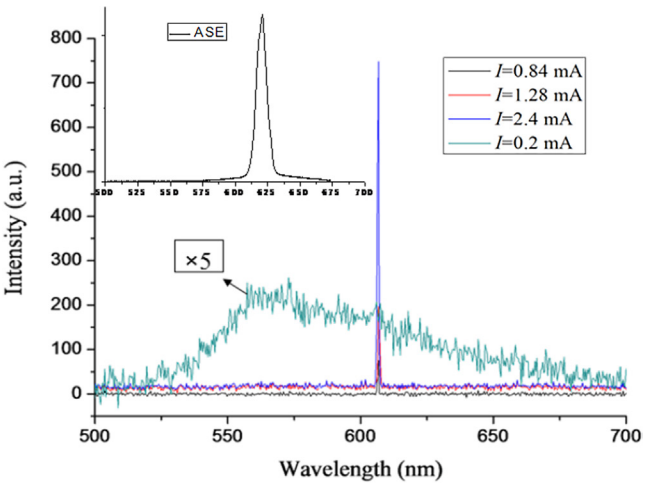

Figure 8. EL spectrum of MEH-PPV QPC microcavity at different currents. The spectrum of spontaneous emission is multiplied by a factor of 5. The inset shows the amplified spontaneous emission from the MEH-PPV waveguide without a PhC structure.

these properties, the resonator plays an important role in light amplification, mode selection and direction collimation. The most common type of laser uses feedback from an optical cavity—a pair of mirrors on either end of the gain medium. It sends light backwards and forwards through the gain medium, being amplified each time by stimulated emission. If the amplification exceeds the losses of the resonator, lasing begins. For our photonic crystal microcavity device, the light transmission direction, mode selection and photon amplification are achieved by the microcavity constructed in the PhCs. According to the characteristics of photonic bandgaps in PhCs and light localization in defect waveguides, the defect modes supported by the point microcavity can only transmit along the waveguide and output vertically from the ITO-glass surface. These light modes are completely determined by the defect structure. In addition, we notice in figure 5 that no matter where light sources are set, those photons matching with the modes supported by the defect are all trapped and accumulate inside the microcavity. That is to say, the output photons from the PhC cavity are not only from the central gain medium in the waveguide, but also from the luminescent medium around the defect, leading to the light amplification and,

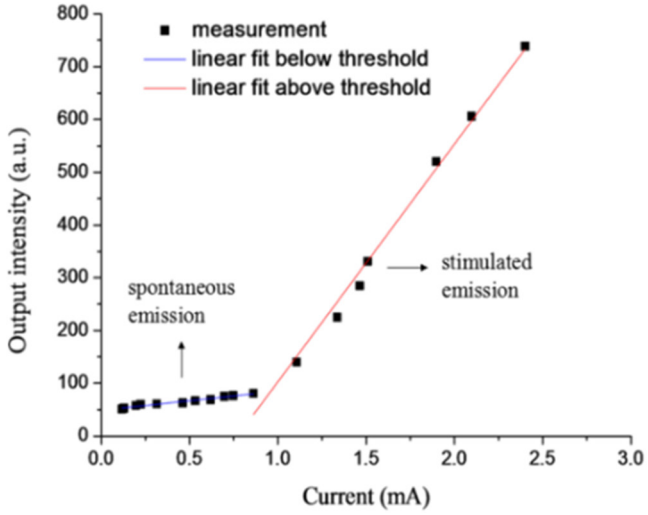

Figure 9. Measured light output-current characteristics of the device.

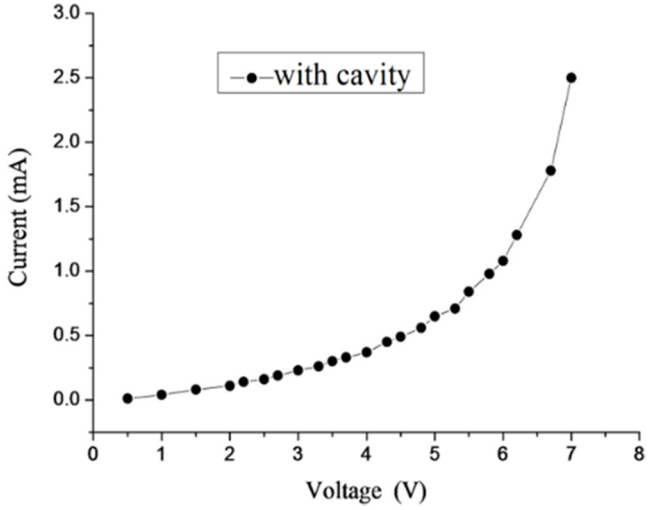

Figure 10. Measured *I–V* characteristics of the organic device with a PhC microcavity.

finally, lasing output. In addition, the quasi-resonator formed between the metal layer and ITO layer in our structure makes the oscillation of light easier.

Figure 10 demonstrates the *I–V* curve of a device with a QPC microcavity. The turn-on voltage reads 5.5 V, which is lower than that without a microcavity in figure 3, while the corresponding current is distinctly higher, especially when the current is above the knee point of 0.8 mA. This phenomenon is very interesting because it has been seldom mentioned in organic PhC lasers before. The possible reason is that the ion implantation occurred during the PhCs fabrication by FIB technology. As we know, ion implantation onto organic polymers is a common tool to modify electrical/optical/magnetic properties through the interaction between energetic ions and electrons of polymers [23–26]. During the FIB process, Ga^+ ion beams are, on one hand, used to etch the micro/nanostructures on MEH-PPV films and, on the other hand, ions doped in polymers enhance the charge-carrier density as well as the mobility, resulting in an increase of MEH-PPV conductivity. Furthermore, Ga^+ ion implantation inevitably induces defect levels in the energy band, thus making the transition $\pi \rightarrow \pi^*$ easier. It helps to achieve the population inversion in organic semiconductors [23].

4. Conclusions

In summary, we designed and fabricated an eight fold quasi-crystal microcavity with a 9-hole-missing point-defect based on the conjugated polymer MEH-PPV at room temperature. Through electrical pumping, the lasing action is observed at $\lambda = 606$ nm with an FWHM of 0.5 nm due to the high-efficiency coupling of spontaneous emission into lasing modes by optical confinement in the quasi-crystal structure. The threshold current of lasing is 0.8 mA. The output intensity of the lasing peak depends on the applied current above the threshold.

Acknowledgments

We acknowledge financial support from the National Science Foundation of China (11204387, 11374378), and the Key Project of Science and Technology from the Ministry of Education of China (212205).

References

[1] Joannopoulos J D, Villeneuve P R and Fan S H 1997 *Nature* **386** 143
[2] Painter O, Lee R K, Scherer A, Yariv A, O'Brien J D, Dapkus P D and Kim I 1999 *Science* **284** 1819
[3] Liu X M, Chung Y, Lin A, Zhao W, Lu K Q, Wang Y S and Zhang T Y 2008 *Laser Phys. Lett.* **5** 904
[4] Wei Y and Sun B 2009 *Laser Phys.* **19** 1252
[5] Liu B-W, Hu M-L, Fang X-H, Wu Y-Z, Song Y-J, Chai L, Wang C-Y and Zheltikov A M 2009 *Laser Phys. Lett.* **6** 44
[6] Ebrahimy M N, Naziri M, Andalib A and Kuzekanani Z D 2016 *Laser Phys.* **26** 066202
[7] BABA Toshihiko 1999 *IEEE J. Sel. Top. Quantum Electron.* **3** 808
[8] Vahala K J 2003 *Nature* **424** 839
[9] Gourdon F, Chakaroun M, Fabre N, Solard J, Cambril E and Yacomotti A M 2012 *Appl. Phys. Lett.* **100** 213304
[10] Tessler N, Denton G J and Friend R H 1996 *Nature* **382** 695
[11] Lončar M, Yoshie T and Scherer A 2002 *Appl. Phys. Lett.* **81** 2680
[12] Park H G, Kim S H, Kwon S H, Ju Y G, Yang J K, Baek J H, Kim S B and Lee Y H 2004 *Science* **305** 1444
[13] Samuel I D W and Turnbull G A 2007 *Chem. Rev.* **107** 1272
[14] Notomi M, Suzuki H and Tamamura T 2001 *Appl. Phys. Lett.* **78** 1325
[15] Tessler N, Medvedev V, Kazes M, Kan S H and Banin U 2002 *Science* **295** 1506
[16] Grivas C and Pollnau M 2012 *Laser Photon. Rev.* **6** 419
[17] Masilamani V, Ibnaouf K H, Alsalhi M S and Yassin O A 2007 *Laser Phys.* **17** 1367
[18] Yang J, Diemeer M B J, Grivas C, Sengo G, Driessen A and Pollnau M 2010 *Laser Phys. Lett.* **7** 650
[19] Wang Y Q, Hu X Y, Xu X S, Cheng B Y and Zhang D Z 2003 *Phys. Rev.* B **68** 165106
[20] Mahler L, Tredicucci A, Beltram F, Walther C, Faist J, Beere H E, Ritchie D A and Wiersma D S 2010 *Nat. Photon.* **4** 165

[21] Arie A and Voloch N 2010 *Laser Photon. Rev.* **4** 355
[22] Yang G J, Chen X, Wang Y Q and Feng S 2013 *Opt. Express* **21** 11457
[23] Das A, Dhara S and Patnaik A 1999 *Nucl. Instrum. Methods Phys. Res.* B **149** 53
[24] Li B M, Cheng L and Zheng Y Y 2010 *J. Polym. Sci.* B **48** 2072
[25] Zhang J Z, Kang J C, Hu P and Meng Q L 2007 *Appl. Surf. Sci.* **253** 5436
[26] Yan S L, Wu H C, Liu X Z, Gao S and Li B M 2008 *Synth. Met.* **158** 1059